

## **Poroelastic properties of jointed rocks: a micromechanics-based analysis**

**Giordano V. S. Lorenci**

Department of Civil Engineering  
Federal University of Rio Grande do Sul – Porto Alegre – RS, Brazil  
giordanosaltie@gmail.com

**Samir Maghous**

Department of Civil Engineering  
Federal University of Rio Grande do Sul – Porto Alegre – RS, Brazil  
samir.maghous@ufrgs.br

**Eduardo Bittencourt**

Department of Civil Engineering  
Federal University of Rio Grande do Sul – Porto Alegre – RS, Brazil  
eduardo.bittencourt@ufrgs.br

### **ABSTRACT**

The formulation of macroscopic poroelastic behavior of a jointed rock is investigated within the framework of a micro-macro approach. The joints are modeled as interfaces and their behavior is modeled by means of generalized poroelastic state equations. Starting from Hill's lemma extended for a jointed medium and extending the concept of strain concentration to relate the joint displacement jump to macroscopic strain, the overall poroelastic constitutive equations for the jointed rock are formulated. The analysis emphasizes the main differences and similarities of the resulting behavior with respect to that characterizing ordinary porous media. It is shown that, unlike ordinary porous media, conditions on the poroelastic parameters of joints are required for the macroscopic drained stiffness to entirely define the poroelastic behavior. This is achieved, for instance, if the joint network is characterized by a unique Biot coefficient.

**Keywords:** jointed rock; poroelasticity; micromechanics,

### **1 INTRODUCTION**

Discontinuities are frequently present at different scales in rock masses and represent a fundamental component of rock deformation and transport of fluid or contaminants through rock masses. Usually referred to as joints, they correspond to zones of small thickness along which the mechanical and physical properties of rock matrix degrade. The presence of joints constitutes the key weak point for stability and safety of many engineering works, such as dam foundations, excavation of tunnels and caverns, oil and gas production, geothermal energy plants, repositories for toxic waste, etc. From transport properties viewpoint, joints within rock masses represent

preferential channels for fluid flow and such, may be contributors to rapid transport of fluid and contaminants through rock masses, particularly when the permeability of the rock matrix is low.

As a consequence, comprehensive constitutive modeling of rocks requires accounting for the poromechanics coupling which occurs at the scale of joints and its implication at the scale of the rock structure. Primarily focus should be on the behavior modeling of the rock material as a porous medium with specific treatment for the coupled hydromechanical coupling governing the joint deformation.

In this context, the main purpose of this paper is to extend the formulation developed in Maghous et al [17] to the situation of a rock with randomly oriented short joints.

## 2 MACROSCOPIC STATE EQUATIONS IN THE CASE OF SATURATED JOINT NETWORK

Considering first the dry case (i.e., in absence of a pressurized fluid), the rock matrix is assumed to be linearly elastic with fourth-order stiffness tensor  $\underline{c}^s$ . As regards the individual behavior of joints, it is assumed that the corresponding elastic domain in  $\mathbb{R}^3$  does not reduce to vector  $\underline{T} = 0$ . Inside the latter domain, the elastic behavior of joints is assumed to remain linear, at least within the range of considered joint strains. The stiffness of joint  $\omega_i$ , relating the stress vector to the displacement jump, is denoted by  $\underline{k}^i$ :

$$\begin{cases} \underline{\underline{\sigma}} = \underline{c}^s : \underline{\underline{\varepsilon}} & \text{in } \Omega \setminus \omega \\ \underline{T} = \underline{\underline{\sigma}} \cdot \underline{n} = \underline{k} : [\underline{\xi}] & \text{along } \omega \end{cases} \quad (1)$$

with  $\underline{n} = \underline{n}_i$  and  $\underline{k} = \underline{k}^i$  along  $\omega_i$ .

The rock matrix fills the domain  $\Omega \setminus \omega$ , where symbol  $\setminus$  stands for the set difference. Note that strains and stresses within the rock medium are defined on the rock matrix domain  $\Omega \setminus \omega$  only, and not on the whole REV. Throughout the paper, symbol  $\langle \cdot \rangle$  denotes the volume average over the rock matrix:

$$\langle \cdot \rangle = \frac{1}{|\Omega_0|} \int_{\Omega \setminus \omega} \cdot \, dV \quad (2)$$

The joints are modelled as interfaces and the associated deformation is described through a phenomenological law  $\underline{T} = \underline{k} \cdot [\underline{\xi}]$  linking the stress vector and the displacement jump. In this context, the joint stiffness  $\underline{k}$  is traditionally evaluated from laboratory tests performed on rock specimen with a single joint. By nature, this phenomenological approach relates the joint stiffness to the geometry and elastic properties of the joint only in a global manner, which can be viewed as a major limitation of the approach.

We now consider the situation where the connected joint network is saturated by a fluid at pressure  $p$  which is assumed to be uniform in the REV. With respect to the dry case, the elastic behavior of the rock matrix is the same as before:  $\underline{\underline{\sigma}} = \underline{c}^s : \underline{\underline{\varepsilon}}$  in  $\Omega \setminus \omega$ . The behavior of the joints is replaced by a poroelastic formulation in order to account for the effect of the fluid pressure on the

relationship between the stress vector acting on the joint and the corresponding relative displacement. The poroelastic state equations for the joints are written in the following form [1, 2]

$$\begin{cases} \underline{T}^n = \underline{\sigma} \cdot \underline{n} = \underline{k} \cdot [\underline{\xi}] + \underline{T}^p \\ \varphi = \frac{p}{m} + \alpha [\underline{\xi}] \cdot \underline{n} \end{cases} \quad \text{along } \omega = \bigcup_i \omega_i \quad (3)$$

where

$$\alpha = \alpha_i, \quad m = m_i, \quad \underline{T}^p = -\alpha_i p \underline{n}_i \quad \text{along } \omega_i \quad (4)$$

Scalar  $\alpha_i$  has the significance of a Biot coefficient for the joint  $\omega_i$  modeled as a generalized porous medium. This means that the displacement jump  $[\underline{\xi}]$  which represents the joint deformation is controlled by the effective stress vector  $\underline{T}^n + \alpha p \underline{n}$ . As regards the second state equation in (3) of the joint, it relates the joint pore change per unit joint surface  $\varphi$  to the fluid pressure  $p$  and the joint displacement jump  $[\underline{\xi}]$ . Scalar  $m_i$  represents the Biot modulus for joint  $\omega_i$ . Physical interpretation as well as identification procedures of the above parameters from appropriate laboratory tests are outlined in [1].

The loading is now characterized by two parameters, namely the macroscopic strain  $\underline{\underline{\epsilon}}$  and the fluid pressure  $p$ . The solution in  $\Omega \setminus \omega$  to this problem defined by the loading mode  $(\underline{\underline{\epsilon}}, p)$  and denoted by (P), is the stress field  $\underline{\sigma}$  in  $\mathfrak{S}$  and the displacement field  $\underline{\xi}$  in  $\mathcal{C}$  related by the state equations of the medium constituents  $\underline{\sigma} = \mathfrak{c}^s : \underline{\underline{\epsilon}}$  in  $\Omega \setminus \omega$  and (3). Due to the linearity of the material behavior expressed in rate form, the superposition principle can be used to decompose problem (P) into two elementary problems (P1) and (P2) respectively defined by the loading  $(\underline{\underline{\epsilon}}, p=0)$  and  $(\underline{\underline{\epsilon}}=0, p)$  as shown in Figure 1. (P1) corresponds to the dry case, whereas (P2) corresponds to pressurized joint network and prevented macroscopic strain.

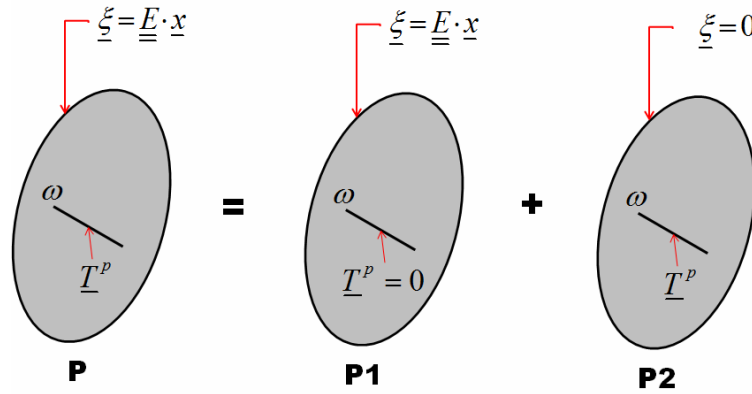


Figure 1: Decomposition of problem (P) into two elementary problems (P1) and (P2).

Let us designate by  $\underline{\xi}_1$ ,  $\underline{\varepsilon}_1$  and  $\underline{\sigma}_1$  the displacement, strain and stress fields in the REV corresponding to problem (P1) and by  $\underline{\xi}_2$ ,  $\underline{\varepsilon}_2$  and  $\underline{\sigma}_2$  the displacement, strain and stress fields in the REV corresponding to problem (P2). The fields solution to problem (P) can simply be obtained as  $\underline{\xi} = \underline{\xi}_1 + \underline{\xi}_2$ ,  $\underline{\varepsilon} = \underline{\varepsilon}_1 + \underline{\varepsilon}_2$  and  $\underline{\sigma} = \underline{\sigma}_1 + \underline{\sigma}_2$ .

## 2.1 First state equation

We introduce the set  $\mathcal{C}$  of displacement fields which are kinematically admissible with  $\underline{\underline{\varepsilon}}$ . By definition, it is the set of displacements fields  $\underline{\xi}'$  continuous and differentiable on  $\Omega \setminus \omega$ . Likewise,  $\mathcal{S}$  denotes the set of statically admissible stress fields  $\underline{\sigma}'$ .

$\underline{\underline{\varepsilon}}$  being prescribed, we consider the elastic problem defined on the REV subjected to the loading defined by the boundary conditions  $\underline{\xi}(x) = \underline{\underline{\varepsilon}} \cdot x$  for  $\forall x \in \partial\Omega_0$ . The solution to this problem is the couple  $(\underline{\sigma}, \underline{\xi})$  in  $\mathcal{S} \times \mathcal{C}$  and complying with (1). Clearly enough,  $\underline{\sigma}$  and  $\underline{\xi}$  linearly depend on the loading parameter  $\underline{\underline{\varepsilon}}$ . This property is usually expressed through the concept of strain concentration tensor, denoted here by the fourth-order tensor  $\mathbb{A}$ . By definition, the term  $\mathbb{A}(x) : \underline{\underline{\varepsilon}}$  represents the strain tensor  $\underline{\varepsilon}$  at point  $x$  corresponding to the load defined previously. In other words,  $\mathbb{A}(x)$  is the link between the local strain  $\underline{\varepsilon}(x)$  in the rock matrix to the macroscopic strain  $\underline{\underline{\varepsilon}}$  applied to the REV. Besides, the strain concentration tensor also relates the local stress  $\underline{\sigma}$  to the macroscopic strain:

$$\underline{\sigma} = \mathbb{C}^s : \mathbb{A} : \underline{\underline{\varepsilon}} \quad (5)$$

The macroscopic stress  $\underline{\underline{\sigma}}$  being defined as the average  $\langle \underline{\sigma} \rangle$ , (5) yields :

$$\underline{\underline{\sigma}} = \mathbb{C}^{\text{hom}} : \underline{\underline{\varepsilon}} \quad \text{with} \quad \mathbb{C}^{\text{hom}} = \langle \mathbb{C}^s : \mathbb{A} \rangle \quad (6)$$

regarding problem (P1), the following relationships thus holds

$$\underline{\underline{\sigma}}_1 = \langle \underline{\sigma}_1 \rangle = \mathbb{C}^{\text{hom}} : \underline{\underline{\varepsilon}} \quad \text{with} \quad \mathbb{C}^{\text{hom}} = \langle \mathbb{C}^s : \mathbb{A} \rangle \quad (7)$$

where the strain concentration tensor  $\mathbb{A}$  relates  $\underline{\varepsilon}_1$  to the loading parameter  $\underline{\underline{\varepsilon}}$  in problem (P)

$$\underline{\varepsilon}_1 = \mathbb{A}(x) : \underline{\underline{\varepsilon}} \quad (8)$$

Due to the presence of the joints the average rule  $\underline{\underline{\mathbb{E}}} = \langle \underline{\underline{\varepsilon}} \rangle$  is not valid in the jointed REV. Accordingly, the average  $\langle \underline{\underline{\mathbb{A}}} \rangle$  of the strain concentration tensor over the rock matrix is not equal to the fourth order identity tensor  $\mathbb{I}$  and thus,  $\mathbb{C}^{\text{hom}}$  is not equal to matrix stiffness of rock matrix  $\mathbb{C}^s$ . More precisely:

$$\langle \underline{\underline{\mathbb{A}}} \rangle = \mathbb{I} - \frac{1}{|\Omega_0|} \int_{\omega} [ \underline{\underline{n}} \otimes \underline{\underline{n}} \otimes \underline{\underline{a}}^n + \underline{\underline{t}} \otimes \underline{\underline{n}} \otimes \underline{\underline{a}}^t + \underline{\underline{t}} \otimes \underline{\underline{n}} \otimes \underline{\underline{a}}^{t'} ] dS \quad (9)$$

The tensors  $\underline{\underline{a}}^n$ ,  $\underline{\underline{a}}^t$  and  $\underline{\underline{a}}^{t'}$  are respectively the concentration tensors for normal and tangential displacement jumps of  $\underline{\underline{\xi}}$ .

Regarding problem (P2),  $\underline{\underline{\Sigma}}_2 = \langle \underline{\underline{\sigma}}_2 \rangle$  represents the macroscopic stress associated with joint interstitial fluid pressure  $p$  which is required to prevent the appearance of any macroscopic strain. In order to evaluate  $\underline{\underline{\Sigma}}_2$ , Hill's lemma (10) is used twice. It is shown [17] that Hill's lemma expressed for jointed media reads:

$$\langle \underline{\underline{\sigma}}' \rangle : \underline{\underline{\mathbb{E}}} = \langle \underline{\underline{\sigma}}' : \underline{\underline{\varepsilon}}' \rangle + \frac{1}{|\Omega_0|} \int_{\omega} \underline{\underline{T}}^m \cdot [ \underline{\underline{\xi}}' ] dS \quad (10)$$

Applying Hill's lemma with the couples  $( \underline{\underline{\sigma}}' = \underline{\underline{\sigma}}_2, \underline{\underline{\xi}}' = \underline{\underline{\xi}}_1 )$  and  $( \underline{\underline{\sigma}}' = \underline{\underline{\sigma}}_1, \underline{\underline{\xi}}' = \underline{\underline{\xi}}_2 )$ , provides the following expression for  $\underline{\underline{\Sigma}}_2$ :

$$\underline{\underline{\Sigma}}_2 = -p \underline{\underline{B}} \quad \text{where} \quad \underline{\underline{B}} = \frac{1}{|\Omega_0|} \int_{\omega} \alpha \underline{\underline{a}}^n dS \quad (11)$$

The first macroscopic state equation is obtained from (7) and (11), by superposition

$$\underline{\underline{\Sigma}} = \underline{\underline{\Sigma}}_1 + \underline{\underline{\Sigma}}_2 = \mathbb{C}^{\text{hom}} : \underline{\underline{\mathbb{E}}} - p \underline{\underline{B}} \quad (12)$$

Similarly to ordinary porous media, the macroscopic strain  $\underline{\underline{\mathbb{E}}}$  is controlled in poroelasticity by an effective Biot stress  $\underline{\underline{\Sigma}} + p \underline{\underline{B}}$ . The tensor  $\underline{\underline{B}}$  can be interpreted as the tensor of Biot coefficients for the jointed medium. The anisotropy introduced by the joint orientation is captured through that of the normal concentration tensor  $\underline{\underline{a}}^n$ .

The limit case of closed joints can be characterized by expressing that the normal component of the relative displacement  $[ \underline{\underline{\xi}} ]$  vanishes, which implies that  $\underline{\underline{a}}^n \rightarrow 0$ . In such a situation, the joint fluid pressure has no effect (i.e.  $\underline{\underline{B}} \rightarrow 0$ ) on the relationship between the macroscopic strain and stress within the elastic domain.

The fundamental difference between the jointed rock and an ordinary porous medium arises when examining how the Biot tensor  $\underline{\underline{B}}$  is connected to the macroscopic elastic tensor of drained

moduli  $\mathbb{C}^{\text{hom}}$ . In the situation where all the joints have the same Biot coefficient, i.e.  $\forall i \alpha_i = \alpha$ . In this situation:

$$\underline{\underline{B}} = \alpha \underline{\underline{1}} : \left( \mathbb{I} - \mathbb{c}^s{}^{-1} : \mathbb{C}^{\text{hom}} \right) \quad (13)$$

If this template is used when writing the full paper, headers and footers will be set automatically.

## 2.2 Second state equation

The complete formulation of the overall poroelastic behavior for the jointed medium is achieved by providing the second macroscopic state equation. The second state equation for the macroscopic poroelastic behavior classically relates the pore volume change to the fluid pressure  $p$  and the macroscopic strain  $\underline{\underline{\epsilon}}$ . In the particular case under consideration, the pore volume change is exclusively due to the joint volume change. For this purpose, we introduce a dimensionless variable called lagrangian porosity change defined as:

$$\Phi = \frac{1}{|\Omega_0|} \int_{\omega} \varphi \, dS \quad (14)$$

Performing the decomposition of  $\underline{\underline{\xi}}$  as  $\underline{\underline{\xi}}_1 + \underline{\underline{\xi}}_2$ , it can be established that [17]:

$$\Phi = \frac{p}{M} + \underline{\underline{B}} : \underline{\underline{\epsilon}} \quad (15)$$

Relationship (15) is the second state equation for jointed porous medium. It constitutes with (12) a set of two equations governing the response of the jointed porous medium.

If all the joints have the same Biot coefficient, i.e.  $\forall i \alpha_i = \alpha$ , the expression of the macroscopic Biot modulus is given by

$$\frac{1}{M} = \frac{1}{\bar{m}} + \frac{1}{\tilde{m}} = \sum_i S_i \frac{1}{m_i} + \alpha \underline{\underline{1}} : \left( \mathbb{c}^s \right)^{-1} : \underline{\underline{B}} \quad (16)$$

where  $\bar{m}$  is the average Biot modulus and  $S_i$  represents the specific area of joint  $\omega_i$ .  $\tilde{m}$  is a scalar which indicate that the response  $\underline{\underline{\xi}}_2$ , and consequently the corresponding jump  $[\underline{\underline{\xi}}_2]$  from loading  $\left( \underline{\underline{\epsilon}} = 0, p \right)$  is proportional to fluid pressure  $p$  [17].

Relationships (13) and (16) show that the overall properties  $M$  and  $\underline{\underline{B}}$  are entirely known once the macroscopic tensor of elastic moduli has been determined. These relationships extend to the situation of jointed rock medium the classical relationships providing the Biot tensor and Biot modulus as functions of solid matrix elasticity  $\mathbb{c}^s$  and dry porous medium elasticity  $\mathbb{C}^{\text{hom}}$  [15].

### 3 APPLICATIONS

Two applications of the micromechanics-based approach to poroelastic properties of jointed rocks are presented in the sequel:

- Rock with short parallel joints;
- Rock with randomly oriented short joints.

#### 3.1 Rock with short parallel joints

We deal now with the situation of a cracked rock. The only heterogeneities considered for the rock medium are short joints (i.e., cracks with load transfer). The analysis presented in the sequel is intended as an extension of classical results established in poroelasticity for cracks which do not transfer stresses.

A convenient way to represent cracks is in the form of oblate spheroids. We introduce for a crack an orthonormal frame  $(\underline{t}, \underline{t}', \underline{n})$ , in which  $\underline{n}$  denotes the normal to the crack plane (Figure 2). The geometry of this oblate spheroid is defined by the crack radius  $a$  and the half opening of the crack  $c$ . The aspect ratio  $X = c/a$  of such a penny-shaped crack is subjected to the condition  $X \ll 1$ . In the continuum micromechanics approach employed herein, a crack represents an inhomogeneity embedded within the rock matrix. We assume for simplicity that the latter is elastically isotropic:

$$\underline{c}^s = 3k^s \mathbb{J} + 2\mu^s \mathbb{K} \quad (17)$$

where  $k^s$  is the bulk modulus and  $\mu^s$  is the shear modulus. The fourth-order tensors  $\mathbb{J}$  and  $\mathbb{K}$  are defined as

$$\mathbb{J} = \frac{1}{3} \underline{1} \otimes \underline{1} \quad ; \quad \mathbb{K} = \mathbb{I} - \mathbb{J} \quad (18)$$

The crack modeled as a short joint (crack with stress transfer) has a stiffness in the form

$$\underline{k} = k_n \underline{n} \otimes \underline{n} + k_t (\underline{t} \otimes \underline{t} + \underline{t}' \otimes \underline{t}') \quad (19)$$

where  $k_n$  and  $k_t$  denote respectively the normal stiffness and shear stiffness.

We consider the situation of a homogeneous rock with parallel cracks defined by the same radius  $a$  and crack aspect ratio  $X$ . The volume fraction of cracks present in the medium is denoted by  $f$ :

$$f = \frac{4}{3} \pi \varepsilon X \quad (20)$$

where  $\varepsilon = \mathcal{N} a^3$  is the crack density parameter of the considered set of parallel cracks introduced by Budiansky and O'Connell [27],  $\mathcal{N}$  being the number of cracks by unit volume.

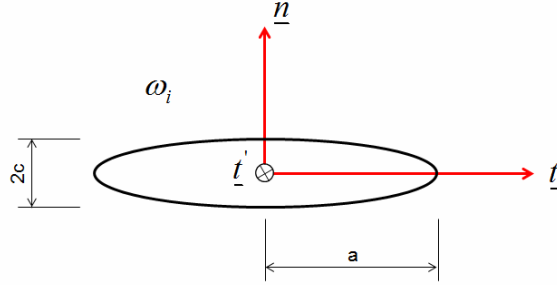


Figure 2: crack as oblate spheroid

Using a Mori-Tanaka scheme, the estimate for the tensor of drained moduli  $\mathbb{C}^{\text{hom}}$  reads:

$$\mathbb{C}^{\text{hom}} = \lim_{X \rightarrow 0} \left( \mathbb{C}^s + f \mathbb{C}^j : \left( \mathbb{I} + \mathbb{P} : (\mathbb{C}^s - \mathbb{C}^j) \right)^{-1} \right) : \left( \mathbb{I} + f \left( \mathbb{I} + \mathbb{P} : (\mathbb{C}^s - \mathbb{C}^j) \right)^{-1} \right)^{-1} \quad (21)$$

where  $\mathbb{P} = \mathbb{P}(X, \underline{n})$  is the Hill tensor associated with the considered crack family. It depends on the aspect ratio  $X$  of the oblate spheroid and its orientation  $\underline{n}$ . The components of the Hill tensor of an oblate spheroid can be found in Handbooks [4, 16]. Tensor  $\mathbb{C}^j$  is related to the crack stiffness

$$\mathbb{C}^j = 3X a (k_n - 4/3 k_t) \mathbb{J} + 2X a k_t \mathbb{K} \quad (22)$$

Since all the cracks have the same poroelastic properties  $(\underline{k}, \alpha, m)$ , the Mori-Tanaka estimate of the Biot tensor reads

$$\underline{\underline{B}} = \alpha \lim_{X \rightarrow 0} f \underline{\underline{1}} : \left( \mathbb{I} + \mathbb{P} : (\mathbb{C}^s - \mathbb{C}^j) \right)^{-1} : \left( \mathbb{I} + f \left( \mathbb{I} + \mathbb{P} : (\mathbb{C}^s - \mathbb{C}^j) \right)^{-1} \right)^{-1} \quad (23)$$

and the Biot modulus estimate can therefore be deduced from that of  $\underline{\underline{B}}$ :

$$\frac{1}{M} = \frac{1}{m} + \alpha \underline{\underline{1}} : \left( \mathbb{C}^s \right)^{-1} : \underline{\underline{B}} \quad (24)$$

In the context of Mori-Tanaka scheme, the non-zero components of tensor  $\mathbb{C}^{\text{hom}}$  estimated by (21) are:

$$\begin{aligned}
 C_{1111} = C_{2222} &= (3k^s + 4\mu^s) \frac{\kappa_2 + \pi(1+16/3\varepsilon)\kappa_1(1-\kappa_1)}{3\kappa_2 + 3\pi\kappa_1(1-\kappa_1) + 4\pi\varepsilon} \\
 C_{3333} &= (3k^s + 4\mu^s) \frac{\kappa_2 + \pi\kappa_1(1-\kappa_1)}{3\kappa_2 + 3\pi\kappa_1(1-\kappa_1) + 4\pi\varepsilon} \\
 C_{1122} = C_{2211} &= (3k^s - 2\mu^s) \frac{\kappa_2 + \pi(\kappa_1 + 8/3\varepsilon)(1-\kappa_1)}{3\kappa_2 + 3\pi\kappa_1(1-\kappa_1) + 4\pi\varepsilon} \\
 C_{1133} = C_{3322} &= (3k^s - 2\mu^s) \frac{\kappa_2 + \pi\kappa_1(1-\kappa_1)}{3\kappa_2 + 3\pi\kappa_1(1-\kappa_1) + 4\pi\varepsilon} \\
 C_{2323} = C_{3131} &= 2\mu^s \frac{4\kappa_3 + \pi(1-\kappa_1)(1+2\kappa_1)}{4\kappa_3 + 16/3\pi\varepsilon(1-\kappa_1) + \pi(1+2\kappa_1)(1-\kappa_1)} \\
 C_{1212} &= \mu^s
 \end{aligned} \tag{25}$$

where the non-dimensional parameters  $\kappa_1$ ,  $\kappa_2$  and  $\kappa_3$  are defined by:

$$\kappa_1 = \frac{3k^s + \mu^s}{3k^s + 4\mu^s} ; \quad \kappa_2 = \frac{3k_n a}{3k^s + 4\mu^s} ; \quad \kappa_3 = \frac{3k_t a}{3k^s + 4\mu^s} \tag{26}$$

Only diagonal components of Biot tensor  $\underline{\underline{B}}$  are not equal to zero:

$$\begin{aligned}
 B_{11} = B_{22} &= 4\alpha\pi\varepsilon \frac{(4/3\kappa_1 - 1)\kappa_1 - 8/9(1-\kappa_1)^2}{3\kappa_2 + 3\pi\kappa_1(1-\kappa_1) + 4\pi\varepsilon} \\
 B_{33} &= \frac{4\alpha\pi\varepsilon}{3\kappa_2 + 3\pi\kappa_1(1-\kappa_1) + 4\pi\varepsilon}
 \end{aligned} \tag{27}$$

Finally, the Biot modulus estimate reads:

$$\frac{1}{M} = \frac{1}{m} + \frac{12\alpha^2\pi\varepsilon}{(3k^s + 4\mu^s)(3\kappa_2 + 3\pi\kappa_1(1-\kappa_1) + 4\pi\varepsilon)} \tag{28}$$

In order to illustrate the solutions obtained, the graphs in Figure 3 show the variation of components from  $\mathbb{C}^{\text{hom}}$ , with respect to the crack density parameter  $\varepsilon$ . In Figure 3, the components  $\mathbb{C}_{ijkl}^{\text{hom}}$  are presented divided by the elasticity modulus of the rock matrix  $E$ . It is assumed that the Poisson's ratio of matrix is equal to 0.25, the volume  $V$  of REV is unitary ( $1 \text{ m}^3$ ) and also that  $\mathcal{N}=1$  (only one fissure in the REV).

The normal and shear stiffness of joint are determined as  $\ell k_n / E$  and  $\ell k_t / E$ , where  $\ell$  is a characteristic dimension given by  $\ell = V^{-2/3} \mathcal{N}^{-1}$ .

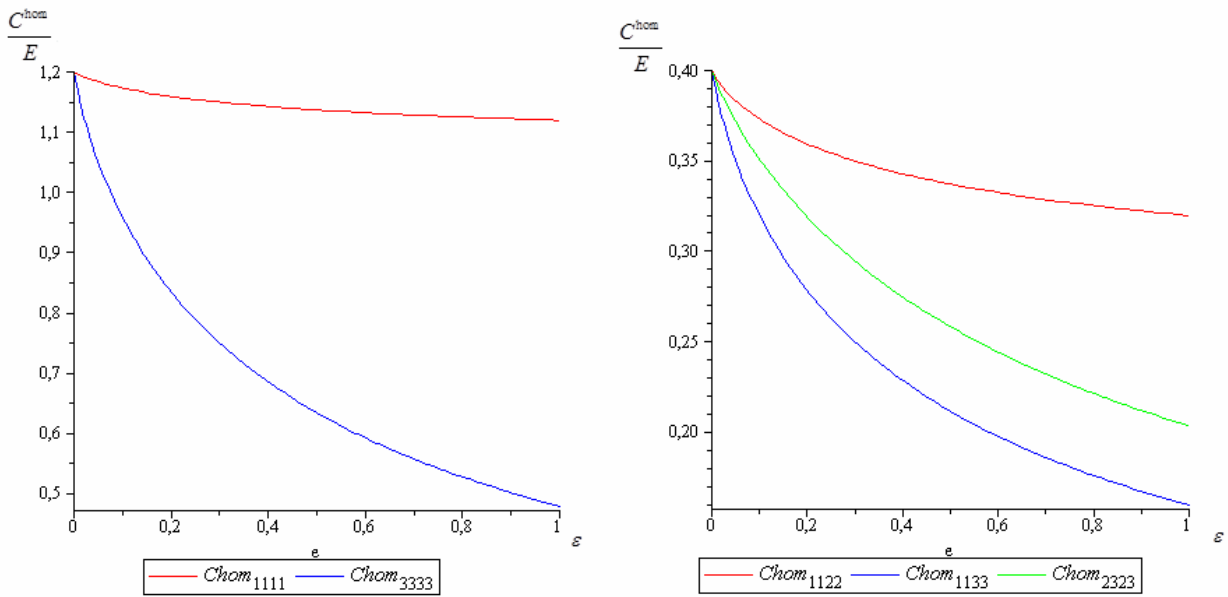


Figure 3: components of  $\mathbb{C}^{hom}$  for a rock medium with short parallel joints

In Figure 4 below, the previous problem is revalued, reducing one thousand times the normal and shear stiffness of the joint, for simulate the case which reduced stresses are transferred across the microcrack.

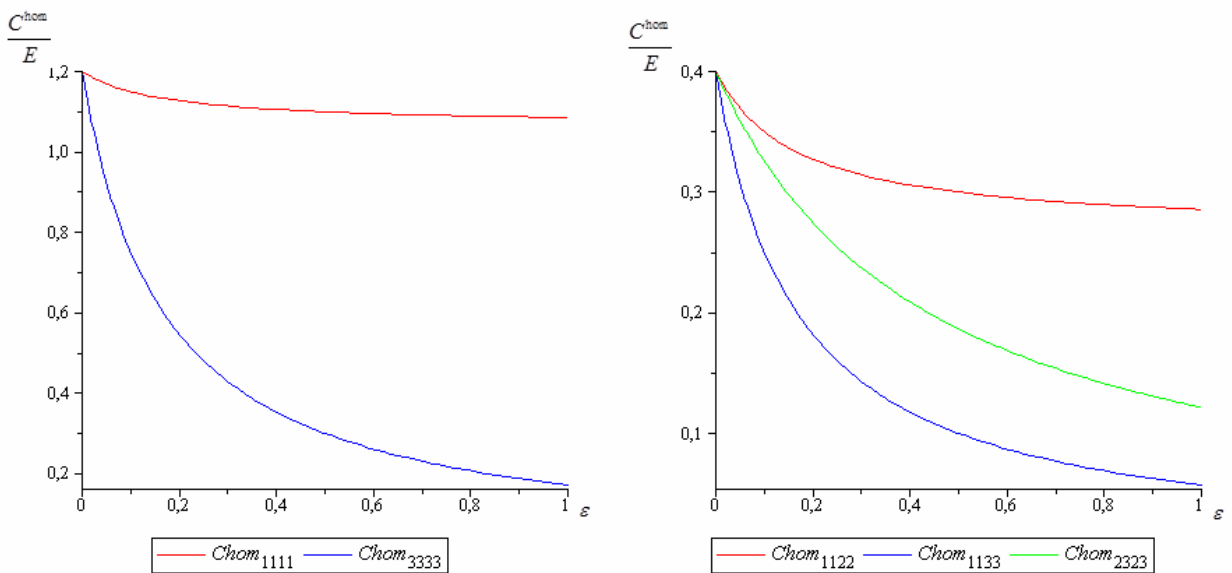


Figure 4: components of  $\mathbb{C}^{hom}$  for a rock medium with short parallel joints, considering  $k_n \ll E$  e  $k_t \ll E$

### 3.2 Rock with randomly oriented short joints

We now examine the situation where the fibers are randomly distributed in the rocky medium. The matrix has an isotropic elastic behavior and the joints are distributed randomly in all directions. The homogenized material will therefore also exhibit an isotropic behaviour.

Following Advani and Tucker [18], the orientation of each fiber is described by a unit vector  $\underline{p}$  whose components are related by two spherical angles  $\theta$  and  $\phi$ . The set of all possible orientations of  $\underline{p}$  is given by describing the unit sphere. The integral over the surface of the sphere, i. e., on the directions of  $\underline{p}$  is given by:

$$\oint dp = \int_0^{\phi=2\pi} \int_0^{\theta=\pi} \sin\theta d\theta d\phi \quad (29)$$

In addition, the orientation in space of a fiber can also be described generally by known orientation distribution function  $\psi(\underline{p})$ . This function is defined as the probability of finding an inclusion between the angles  $\theta_1$  and  $(\theta_1 + d\theta)$ , and  $\phi_1$  and  $(\phi_1 + d\phi)$ :

$$P(\theta_1 \leq \theta \leq \theta_1 + d\theta, \phi_1 \leq \phi \leq \phi_1 + d\phi) = \psi(\theta_1, \phi_1) \sin\theta_1 d\theta d\phi \quad (30)$$

If  $dN$  refers to the volume density of cracks, the fraction of fibers  $df$  can be written as:

$$df = \frac{4}{3} \pi a^2 c dN = \frac{X}{3} a^3 N \sin(\theta) d\phi d\theta \quad (31)$$

Finally, it should be observed that the approach described in section 3.1 can be extended to the case of a rock with randomly (isotropic) oriented short joints by integration over the crack orientations:

$$\mathbb{C}^{\text{hom}} = \lim_{X \rightarrow 0} \left( \overline{\mathbb{C}^s + \mathbb{C}^j : (\mathbb{I} + \mathbb{P} : (\mathbb{C}^s - \mathbb{C}^j))^{-1}} \right) : \left( \overline{\mathbb{I} + (\mathbb{I} + \mathbb{P} : (\mathbb{C}^s - \mathbb{C}^j))^{-1}} \right)^{-1} \quad (32)$$

where symbol  $\overline{\mathcal{Q}}$  denotes the integral over the spherical angular coordinates  $\theta \in [0, \pi]$  and  $\phi \in [0, 2\pi]$ :

$$\overline{\mathcal{Q}} = \int_0^{\pi} d\theta \int_0^{2\pi} \frac{4\pi a^3}{3} X N \mathcal{Q}(\theta, \phi) \frac{\sin\theta}{4\pi} d\phi \quad (33)$$

In the context of Mori-Tanaka scheme, the non-zero components of tensor  $\mathbb{C}^{\text{hom}}$  estimated by (22) are:

$$\begin{aligned}
C_{1111}^{\text{hom}} = C_{2222}^{\text{hom}} &= \frac{3\beta_1}{\beta_2\beta_3} (3k^s + 4\mu^s) (81k^{s2}\pi^2\mu^{s2} + 234k^{s2}a\epsilon\pi^2\mu^{s2} + 216k^{s2}a^2\epsilon\pi\mu^s k_t + \\
&108k^{s2}\pi\mu^s a k_t + 81k^{s2}\pi\mu^s a k_n + 72k^{s2}a^2\epsilon\pi\mu^s k_n + 108k^{s2}k_n k_t a^2 + 210k^s a\epsilon\pi^2\mu^{s3} + \\
&81k^s\pi^2\mu^{s3} + 162k^s\pi\mu^{s2} a k_n + 120k^s a^2\epsilon\pi\mu^{s2} k_n + 360k^s a^2\epsilon\pi\mu^{s2} k_t + 180k^s a\pi\mu^{s2} k_t + \\
&288k^s a^2\mu^s k_n k_t + 44a\epsilon\pi^2\mu^{s4} + 18\pi^2\mu^{s4} + 96a^2\epsilon\pi\mu^{s3} k_t + 48\pi a\mu^{s3} k_t + 72\pi a\epsilon\mu^{s3} k_n \\
&+ 32a^2\epsilon\pi\mu^{s3} k_n + 192a^2\mu^{s2} k_n k_t) \\
C_{1122}^{\text{hom}} = C_{2211}^{\text{hom}} &= \frac{3\beta_1}{\beta_2\beta_3} (648k^{s2}a^2\mu^{s2} k_n k_t - 384a^2\mu^{s3} k_n k_t + 243k^{s3}\pi^2\mu^{s2} + 81k^s\pi^2\mu^{s3} \\
&- 36\pi^2\mu^{s5} + 324k^{s3}a^2 k_n k_t - 108k^s\pi^2\mu^{s4} - 96\pi a\mu^{s4} k_t - 144\pi a\mu^{s4} k_n + \\
&216k^{s3}a^2\epsilon\pi\mu^s k_n + 648k^{s2}a^2\epsilon\pi\mu^{s2} k_n - 648k^{s2}a^2\epsilon\pi\mu^{s2} k_t - 216k^{s3}a^2\epsilon\pi\mu^s k_t - \\
&576k^s a^2\epsilon\pi\mu^{s3} k_t + 243k^{s3}a\pi\mu^s k_n + 54k^{s3}a\epsilon\pi^2\mu^{s2} - 36k^s a\epsilon\pi^2\mu^{s4} + 128a^2\epsilon\pi\mu^{s4} k_n \\
&- 128a^2\epsilon\pi\mu^{s4} k_t + 324k^{s3}a\pi\mu^s k_t - 16a\epsilon\pi^2\mu^{s5} + 324k^{s2}a\pi\mu^{s2} k_n + 324k^{s2}a\pi\mu^{s2} k_t - \\
&216k^s a\pi\mu^{s3} k_t - 108k^s a\pi\mu^{s3} k_n + 576k^s a^2\epsilon\pi\mu^{s3} k_n) \\
C_{1212}^{\text{hom}} &= \frac{3\beta_1\mu^s}{\beta_2} (9k^s\pi\mu^s + 12k^s a k_t + 6\pi\mu^{s2} + 16a\mu^s k_t) \\
C_{1313}^{\text{hom}} = C_{2323}^{\text{hom}} &= \frac{3\mu^s (9k^s\pi\mu^s + 12k^s a k_t + 6\pi\mu^{s2} + 16a\mu^s k_t)}{27k^s\pi\mu^s + 36k^s a k_t + 24k^s a\epsilon\pi\mu^s + 48\mu^s a k_t + 18\pi\mu^{s2} + 32a\epsilon\pi\mu^{s2}} \quad (34) \\
C_{1133}^{\text{hom}} = C_{3311}^{\text{hom}} = C_{2233}^{\text{hom}} = C_{3322}^{\text{hom}} &= \frac{3\beta_1}{\beta_3} (3k^s - 2\mu^s) \\
C_{3333}^{\text{hom}} &= \frac{3}{\beta_3} (3k^s + 4\mu^s) (3k^s a k_n + 12k^s a\epsilon\pi\mu^s + 3k^s\pi\mu^s + 4a\mu^s k_n + \pi\mu^{s2})
\end{aligned}$$

where the parameters  $\beta_1$ ,  $\beta_2$  and  $\beta_3$  are defined by:

$$\begin{aligned}
\beta_1 &= 3k^s\pi\mu^s + 3k^s a k_n + 4\mu^s a k_n + \pi\mu^{s2} \\
\beta_2 &= 108k^{s2}\pi\mu^s a k_t + 72k^{s2}a^2\epsilon\pi\mu^s k_t + 108k^{s2}k_n k_t a^2 + 81k^{s2}\pi\mu^s a k_n + 72k^{s2}a^2\epsilon\pi\mu^s k_n \\
&+ 126k^{s2}a\epsilon\pi^2\mu^{s2} + 81k^{s2}\pi^2\mu^{s2} + 81k^s\pi^2\mu^{s3} + 288k^s a^2\mu^s k_n k_t + 192k^s a^2\epsilon\pi\mu^s k_n \\
&+ 192k^s a^2\epsilon\pi\mu^s k_t + 180k^s a\pi\mu^{s2} k_t + 162k^s\pi\mu^{s2} a k_n + 228k^s a\epsilon\pi^2\mu^{s3} + 18\pi^2\mu^{s4} + \\
&48\pi a\mu^{s3} k_t + 80a\epsilon\pi^2\mu^{s4} + 192a^2\mu^{s2} k_n k_t + 128a^2\epsilon\pi\mu^{s3} k_t + 128a^2\epsilon\pi\mu^{s3} k_n + 72a\pi\mu^{s3} k_n \\
\beta_3 &= 36k^{s2}a\epsilon\pi + 27k^s\pi\mu^s + 27k^s\pi k_n + 60k^s a\epsilon\pi\mu^s + 36\mu^s a k_n + 9\pi\mu^{s2} + 16a\epsilon\pi\mu^{s2}
\end{aligned} \quad (35)$$

Again, only diagonal components of Biot tensor  $\underline{B}$  are not equal to zero:

$$\begin{aligned}
B_{11}^{\text{hom}} = B_{22}^{\text{hom}} &= \frac{4a\epsilon\pi\alpha}{\beta_2} (9k^{s2} + 15k^s\mu^s + 4\mu^{s2}) \\
B_{33}^{\text{hom}} &= \frac{4a\epsilon\pi\alpha}{\beta_2} (9k^{s2} + 6k^s\mu^s - 8\mu^{s2})
\end{aligned} \quad (36)$$

The Biot modulus estimate reads:

$$\frac{1}{M} = \frac{1}{m} + \frac{12a\varepsilon\pi\alpha^2}{\beta_2} (3k^s + 4\mu^s) \quad (37)$$

Again, in order to illustrate the solutions obtained, the graphs in Figure 5 show the variation of components from  $\mathbb{C}^{\text{hom}}$ , with respect to the crack density parameter  $\varepsilon$ . We use the same data given in section 3.1.

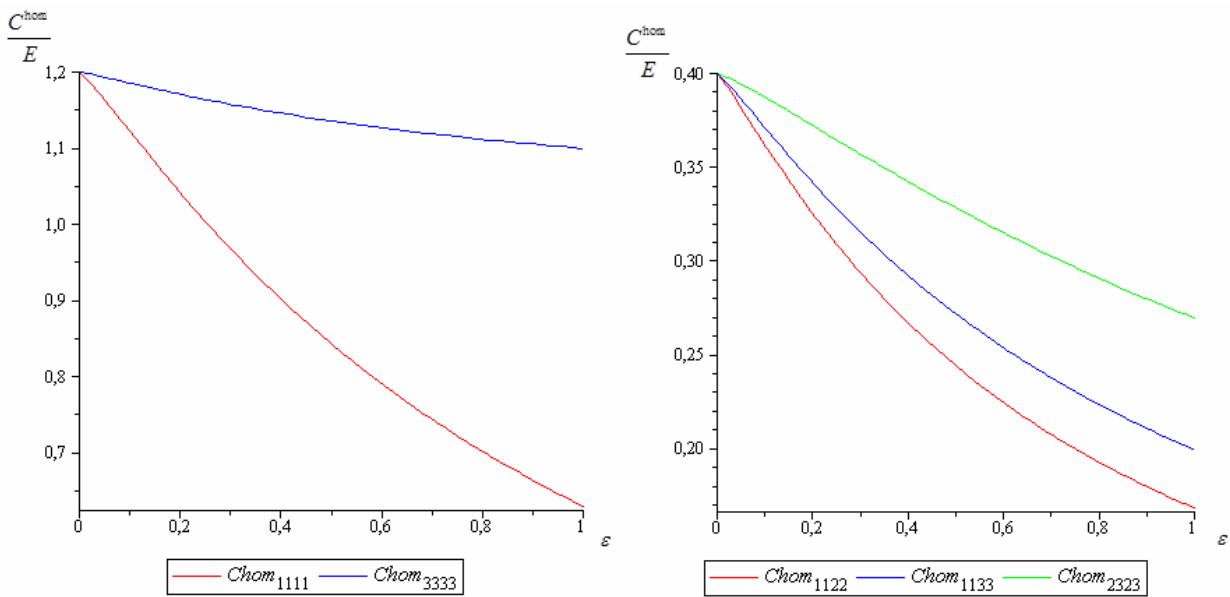


Figure 5: components of  $\mathbb{C}^{\text{hom}}$  for a rock medium with randomly oriented short joints

As in section 3.1, in the Figure 6 below, the previous problem is revalued, reducing one thousand times the normal and shear stiffness of the joint, simulating the case which reduced stresses are transferred across the microcrack.

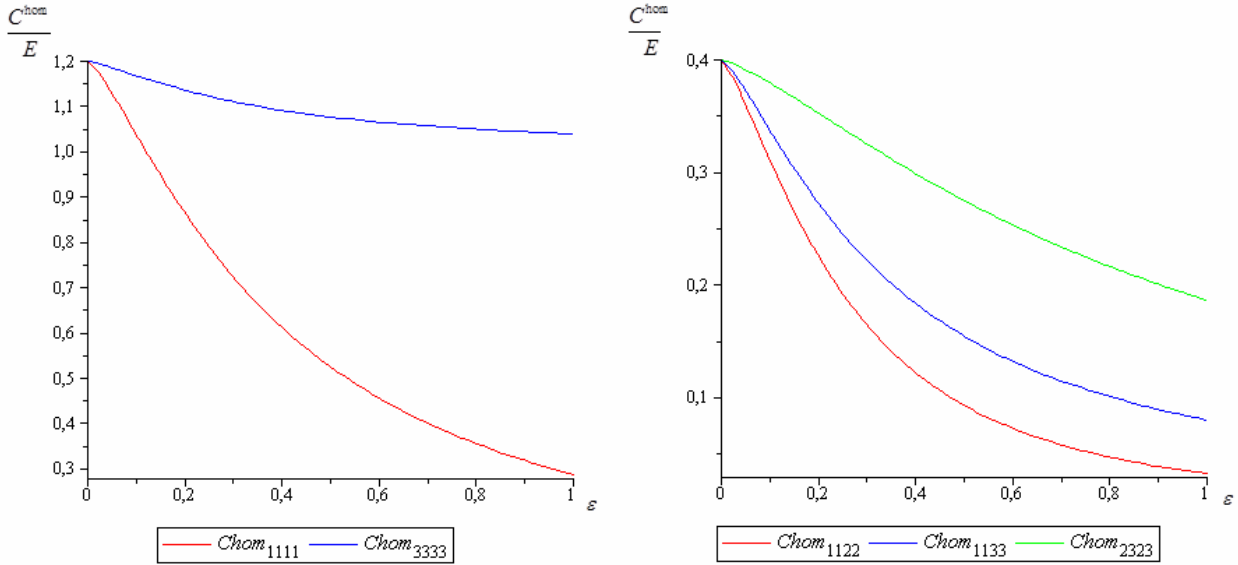


Figure 6: components of  $\mathbb{C}^{\text{hom}}$  for a rock medium with randomly oriented short joints, considering  $k_n \ll E$  e  $k_t \ll E$

#### 4 CONCLUSION

The micromechanical analysis of the behavior of rocks with fluid saturated joint network has been presented.

Extending the concept of strain concentration tensor to jointed media, the reasoning relies upon the formulation of Hill lemma for such materials and the introduction of strain concentration tensors for the displacement jump along the joints, modeled as interfaces. The two state equations for the rock medium with a fluid saturated connected joint network have been formulated. They can be viewed as an extension of the poroelasticity Biot theory to such materials. In the situation when all the joints are characterized by the same Biot coefficient, it is established that the homogenized Biot coefficient  $\underline{B}$  and Biot modulus  $M$  are related to the homogenized tensor of drained moduli  $\mathbb{C}^{\text{hom}}$  by Eqs. (13) and (16), extending to the case of jointed rocks the classical relationships available for ordinary porous media. From a practical viewpoint, this means that the determination of poroelastic properties reduces to elastic homogenization in the dry case.

The displacement field solution to the poroelastic concentration problem stated on the REV is *a priori* required for the determination of the homogenized Biot coefficient  $\underline{B}$  and Biot modulus  $M$ . Alternatively their determination can also result from solving the two elementary problems: *a*) problem (P1), corresponding to the dry case and which solution provides field  $\underline{a}^n$ , and consequently tensor  $\underline{B}$  by (11), and, *b*) problem (P2), corresponding to pressurized joint space with prevented macroscopic strain, which provides field  $[\underline{\xi}_2]$  along the joints.

Finally, results are presented for two cases of fissured rocks. First, we presents the case of a rock medium containing short parallel joints. In Section 3.2, this result is extended for a rock medium with randomly oriented short joints.

A numerical solution, by applying the concept of cohesive interface via finite element method is currently under development, to allow the comparison of results obtained by analytical solutions.

## REFERENCES

- [1] Bart M, Shao JF, Lydzba D, Haji-Sotoudeh M. Coupled hydromechanical modeling of rock fractures under normal stress. *Can Geotech J* 2004; 41:686-697.
- [2] Dormieux L, Maghous S, Kondo D, Shao JF. Macroscopic poroelastic behavior of a jointed rock. In: Auriault et al., editors. *Proceedings of the 2nd Biot conference, poromechanics II*, Grenoble, 2002. p. 179-183.
- [3] Zaoui A. Continuum micromechanics: survey. *J Eng Mech ASCE* 2002; 128:808-816.
- [4] Nemat-Nasser S, Horii H. *Micromechanics: overall properties of heterogeneous materials*. Amsterdam: North-Holland; 1993.
- [5] Deudé V, Dormieux L, Kondo D, Maghous S. Micromechanics approach to nonlinear poroelasticity: application to cracked rocks. *J Eng Mech ASCE* 2002; 128: 848-855.
- [6] Hill R. The essential structures of constitutive laws for metal composites and polycrystals. *J Mech Phys Solids* 1967; 15:79-95.
- [7] Budiansky B., O'Connell RJ. Elastic moduli of cracked solid. *Int J Solids Struct* 1976; 12:81-97.
- [8] Pensée V, Kondo D, Dormieux L. Micromechanical analysis of anisotropic damage in brittle materials. *J Eng Mech ASCE* 2002; 128:889-897.
- [9] Dormieux L, Kondo D, Ulm F-J. A micromechanical analysis of damage propagation in fluid-saturated cracked media. *Comptes Rendus Mécanique*, 2006; 334:440-446.
- [10] Eshelby JD. The determination of the elastic field of an ellipsoidal inclusion and related problem. *Proc. Roy Soc London* 1957; A241:376-396.
- [11] de Buhan P, Maghous S. Comportement élastique non linéaire macroscopique d'un matériau comportant un réseau de joints. *Comptes Rendus Acad Sci Paris* 1997; 324(IIb):209-218.
- [12] Maghous S, de Buhan P, Dormieux L, Garnier D. Comportement élastoplastique homogénéisé d'un milieu rocheux fracturé. *Comptes Rendus Acad Sci Paris* 2000; 328(IIb) :701-708.
- [13] Maghous S, Bernaud D, Fréard J, Garnier D. Elastoplastic behavior of jointed rock masses as homogenized media and finite element analysis. *Int J Rock Mech Min Sci* 2008;45:1273-1286.
- [14] Dormieux L, Kondo D, Ulm FJ. *Microporomechanics*. Chichester: Wiley; 2006.
- [15] Auriault JL, Sanchez-Palencia E. Etude du comportement macroscopique d'un milieu poreux saturé déformable. *J Méc* 1977;16: 575-603.
- [16] Mura T. *Micromechanics of defects in solids*, 2nd edition. Dordrecht: Martinus Nijhoff Publishers; 1987.
- [17] Maghous S, Dormieux L, Kondo D, Shao JF. Micromechanics approach to poroelastic behavior of a jointed rock. *International Journal for Numerical and Analytical Methods in Geomechanics* 2013, vol 37: 111-129.
- [18] Advani, S G; Tucker, C L. The use of tensors to describe and predict fiber orientation in short fiber composites. *Journal of Rheology*, vol. 31, n. 8, p. 751-784. 1987.